

Negative Refraction Gives Rise to the Klein Paradox

Durdu Ö. Güney*

*Department of Electrical and Computer Engineering, University of California, San Diego,
9500 Gilman Dr., La Jolla, California, 92093-0409*

*Department of Mathematics, University of California, San Diego, 9500 Gilman Dr.,
La Jolla, California, 92093-0112*

dguney@ucsd.edu

David A. Meyer

*Department of Mathematics, University of California, San Diego, 9500 Gilman Dr.,
La Jolla, California, 92093-0112*

dmeyer@math.ucsd.edu

Abstract

Electromagnetic negative refraction in metamaterials has attracted increasingly great interest, since its first experimental verification in 2001. It potentially leads to the applications superior to conventional devices including compact antennas for mobile stations, imaging beyond the diffraction limit, and high-resolution radars, not to mention the anomalous wave propagation in fundamental optics. Here, we report how metamaterials could be used to simulate the “negative refraction of spin-zero particles interacting with a strong potential barrier”, which gives rise to the Klein paradox—a counterintuitive relativistic process. We address the underlying physics of analogous wave propagation behaviours in those two entirely different domains of quantum and classical.

1. Introduction

About thirty years after Veselago’s theoretical prediction¹, an effective left-handed material (LHM) was proposed, consisting of a periodic array of split ring resonators (SRRs) and continuous wires, which manifests refractive index $n < 0$ for a certain frequency region^{2–3}. First, experimental verification of LHM was achieved in 2001 in San Diego⁴. Subsequent efforts pushed the limits to telecom band and even to visible spectrum^{5–9}. In an entirely different domain, here we report how the LHMs could indeed simulate the negative refraction of spin-zero particles interacting with a strong potential barrier. Hence, they give rise to the Klein paradox—a counterintuitive phenomenon in relativistic quantum mechanics. We explain the underlying physics of the similar wave propagation behaviors in the Klein-Gordon and the Maxwellian pictures. Our work has implications to the analog quantum simulations of many exotic phenomena in quantum electrodynamics with relatively simple optical benchtop experiments and metamaterial designs on demand.

By taking the three spatial coordinates into account¹³, the generation of scalar particles in the presence of a strong Klein step potential^{10–12} has been considered. To the best of our knowledge, such a two-dimensional (2D) scattering from a semi-infinite Klein step potential has not been considered. Hence, the negative refraction is treated explicitly here first, inspired by the works about its optical counterpart, LHM^{1,14–16}. It is amazing that the 2D case not only verifies the Klein paradox existing in one dimension, but it also shows the negative refraction of matter waves. Besides, in the territory of electronics, also inspired by LHMs, negative refraction was recently predicted theoretically in a *Science* paper by Cheianov et al.¹⁷ in a monolayer of graphite (graphene). Graphene not only leads to the focusing of electrons¹⁷ similar to the perfect optical lens, but also exhibits the Klein paradox^{18–19}. However, no link between the Klein paradox and the negative refraction has been found in graphene.

2. Left Handed Material

To achieve our goal, we will first illustrate some relevant features of the refraction at the interface between a positive refractive index material (PIM) and effectively LHM. We will consider the Klein paradox later.

In Fig. 1, we show the negative refraction^{1,14–16} of an obliquely incident Gaussian wavepacket, with a center frequency of 5GHz, at the interface between semi-infinite PIM ($z < 0$) and NIM (i.e., LHM or negative index material) ($z > 0$) media. From a simple SRR (common magnetic constitute of LHMs to provide the negative permeability) and wire pair-based LHM model^{2,3}, we estimated $\epsilon = -4.76$, $\mu = -1.222$, and $n = -2.412$ at the center frequency. Arrows indicate an arbitrary wavevector component, \mathbf{K}_L (L for LHM), in the incident wavepacket (see the bottom left quadrant of the figure) and the corresponding wavevector components, \mathbf{Q}_L and \mathbf{K}'_L , in the transmitted (bottom right quadrant) and reflected (top left quadrant) wavepackets, respectively. Arrows are drawn perpendicular to their respective wavefronts (i.e., \mathbf{K}_L , for example, corresponds to a uniform plane wave component of the incident wavepacket in the bottom left quadrant). Below, we briefly describe why negative refraction occurs under the settings of Fig. 1.

Wave vector, \mathbf{K}_L , of the electric field incident on the dispersive LHM from vacuum makes an angle, Θ_i , with the normal to the boundary located at $z = 0$. Because the individual incident electric field is a plane wave and linearly polarized along the y -axis, its wave vector lies in the xz -plane. That is

$$E(\mathbf{r}, t) = e^{i(\mathbf{K}_L \cdot \mathbf{r} - \omega t)}, \quad (1)$$

with unit amplitude. It can be shown by the phase matching condition and causality for the refracted wave that the transmitted wave vector \mathbf{Q}_L is

$$\mathbf{Q}_L = K_{Lx} \hat{\mathbf{x}} + \sigma \sqrt{n^2 K_L^2 - K_{Lx}^2} \hat{\mathbf{z}}. \quad (2)$$

$\sigma = +1$ for the positive index medium and -1 for the LHM¹⁴. From the definition of group velocity for isotropic, low loss materials, the refracted beam has the group velocity

$$\mathbf{V}_g = \frac{\mathbf{Q}_L \sigma c}{Q_L n_g}, \quad (3)$$

where c is the light speed and n_g is the group index, which is by causality always greater than unity¹⁵. Thus the group velocity is always antiparallel to the phase velocity of the refracted wave for $\sigma = -1$. Since the time-averaged energy flux $\langle \mathbf{S} \rangle = \langle u \rangle \mathbf{V}_g$ ¹⁶, where $\langle u \rangle$ is the time-averaged energy density, it is clear from equations (2) and (3) and by causality that the incident wave should undergo negative refraction.

Field transmission (τ_L) and reflection (ρ_L) coefficients for LHM can be determined by matching the electric and magnetic fields at the interface between right and left handed media. That gives,

$$\tau_L = \frac{2\mu K_{Lz}}{\mu K_{Lz} + Q_{Lz}} \quad (4)$$

$$\rho_L = \frac{\mu K_{Lz} - Q_{Lz}}{\mu K_{Lz} + Q_{Lz}}. \quad (5)$$

where μ is the effective permeability of the LHM. Power transmission and reflection coefficients can be obtained from the average energy flux $\langle \mathbf{S} \rangle = (c/8\pi)\Re[\mathbf{E} \times \mathbf{H}^*]$. Thus we have, respectively,

$$T_L = \frac{|\tau_L|^2 Q_{Lz}}{\mu K_{Lz}}, \quad (6)$$

$$R_L = |\rho_L|^2. \quad (7)$$

3. Klein Paradox

Now, we turn our attention to the Klein paradox. Although the nonrelativistic quantum mechanics of the scattering of a quantum particle is straightforward, the relativistic case displays quite peculiar situation called the Klein Paradox^{11,20-21}. In the following we discuss 2D scattering of a particle from a Klein step potential and consider some of these peculiarities, which include transmission through strong potential barrier, pair production, negative transmission and negative refraction.

We consider a spin-0 particle with momentum P and energy $E = (P^2 c^2 + m^2 c^4)^{1/2}$, which is governed by the KG equation,

$$[\mathbf{E} - V(\mathbf{r})]^2 |\Psi\rangle = (c^2 \mathbf{P}^2 + m^2 c^4) |\Psi\rangle, \quad (8)$$

where m is the mass of the particle.

In Fig. 2, we show the negative refraction of an obliquely incident Gaussian beam of those spin-zero particles at the boundary of a strong potential, $V(\mathbf{r})$, which is assumed to be 0 on the incident side and described by a 2D Klein step potential, $V(\mathbf{r}) = V$ for $z > 0$. \mathbf{K}_K represents the wave vector for an arbitrary plane wave component in the incident flux (see the bottom left quadrant of the figure), while \mathbf{Q}_K and \mathbf{K}'_K indicate the corresponding wave vectors for transmitted (bottom right quadrant) and reflected (top left quadrant) plane waves, respectively. The angle between \mathbf{K}_K and the boundary normal is Θ_i . As we demonstrate below, the directions of group (\mathbf{V}_g) and phase (\mathbf{V}_p) velocities for the transmitted beam are antiparallel.

In the position representation, equation (8) becomes

$$\{[i\hbar\partial_t - V(\mathbf{r})]^2 + c^2\hbar^2\nabla^2 - m^2c^4\}\Psi(\mathbf{r}, t) = 0. \quad (9)$$

For $z < 0$, consider the individual positive energy plane wave component, in the incident wavepacket in Fig. 2, which is of the form

$$\Phi(\mathbf{r}, t) = e^{i(\mathbf{K}_K \cdot \mathbf{r} - Et/\hbar)}. \quad (10)$$

Note that equation (10) is similar to equation (1) given for the y -polarized electric field.

We look for the solution of the form

$$\Psi(\mathbf{r}) = \phi(-z)[e^{-iEt/\hbar}(e^{i\mathbf{K}_K \cdot \mathbf{r}} + \rho_K e^{i\mathbf{K}'_K \cdot \mathbf{r}})] + \phi(z)\tau_K e^{-iEt/\hbar} e^{i\mathbf{Q}_K \cdot \mathbf{r}}, \quad (11)$$

where $\phi(z)$ is the unit step function. Substitution of equation (11) into equation (9) and satisfying the phase matching condition, $K_{Kx} = K'_{Kx} = Q_{Kx}$, yields

$$E^2 = c^2\hbar^2 K_K^2 + m^2c^4, \quad z < 0 \quad (12)$$

$$c^2\hbar^2 Q_K^2 = (E - V)^2 - m^2c^4, \quad z > 0. \quad (13)$$

We can analyse equation (13) by considering three cases. If the potential V is weak, such that it is less than $E - mc^2$, then Q_K has to be real. For the intermediate case, where $E - mc^2 < V < E + mc^2$, Q_K is purely imaginary, so the transmitted field is damped.

We concentrate on the strong potential case, that is $V > E + mc^2$. Note that we again have real Q_K . Even when the energy of the incident particle is less than the height of the potential, the transmitted particle doesn't necessarily undergo any attenuation. This is a classically (also in nonrelativistic quantum mechanics) forbidden situation.

The question thus naturally arises: What is the direction of the momentum of the transmitted wave, or \mathbf{Q}_K , for the strong potential case? Since $E(\mathbf{Q}_K) = E(Q_K)$ in equation (13), for the group velocity of the transmitted wave we have

$$\mathbf{V}_g = \frac{\hbar c \mathbf{Q}_K}{E - V}. \quad (14)$$

If equation (14) is not considered for the moment, to satisfy the phase matching condition at the interface, incoming wave in equation (10) should either propagate along the vector \mathbf{Q}_K in Fig. 2 or along a vector, which is directed away from the boundary and has the same tangential component with that of the incoming (\mathbf{K}_K) and reflected waves (\mathbf{K}'_K) (i.e., mirror symmetry of \mathbf{Q}_K multiplied by -1). Since the denominator of equation (14) is negative, however, the group velocity \mathbf{V}_g and the wave vector \mathbf{Q}_K must be antiparallel. Therefore,

we must pick the former path of propagation (i.e., along \mathbf{Q}_K). Otherwise, since the group velocity is the velocity of the moving wave packet, the causality is violated by allowing an incoming wavepacket from positive- z side. Thus, it is clear that we observe negative refraction in Fig. 2 analogous to LHMs.

Since the momentum, or \mathbf{Q}_K , of the transmitted wave is a function of the energy of the incident particle E , we can write equation (13) in terms of its components as

$$c^2\hbar^2Q_{K_z}^2 = c^2\hbar^2K_{K_x}^2 - 2EV + V^2. \quad (15)$$

Remember that we found Q_K to be real in the strong potential case, where $E < V$ and we know that $Q_{K_x}^2 = K_{K_x}^2$ is real positive. Therefore, we immediately conclude from equation (15) that Q_{K_z} can be real as well as purely imaginary, even though Q_K is real. Now we closely examine the condition which makes Q_{K_z} either real or purely imaginary. To achieve that we define the excess potential as

$$\Delta V \equiv V - E - mc^2. \quad (16)$$

If we substitute V in equation (16), into equation (15) we obtain

$$c^2\hbar^2Q_{K_z}^2 = 2mc^2(\Delta V) + (\Delta V)^2 - c^2\hbar^2K_{K_x}^2. \quad (17)$$

Since ΔV is arbitrarily chosen, for a given incident particle with mass m , it is interesting that the stronger the potential the more momentum transfer to the z -component of the transmitted wave occurs without any damping. As we increase the height of the potential step, keeping m and K_{K_x} the same, the angle of refraction approaches zero. However, for the relatively weaker potential such that $0 < \Delta V < -mc^2 + (c^2\hbar^2K_{K_x}^2 + m^2c^4)^{1/2}$, the transmitted wave is damped. Interestingly this does not occur in the 1D scattering from a strong potential of the same kind. First, this could be easily understood from equation (17) by setting $K_{K_x} = 0$, so that Q_{K_z} never becomes purely imaginary. Second, equation (17) also states that pair production in 2D scattering requires an additional potential of $\Delta V = -mc^2 + (c^2\hbar^2K_{K_x}^2 + m^2c^4)^{1/2}$ for given m and K_{K_x} , compared to one-dimensional (1D) scattering.

The expressions for ρ_K and τ_K in equation (11) are determined by imposing the boundary conditions on $\Psi(\mathbf{r})$ and $\partial_z\Psi(\mathbf{r})$ at the interface, $z = 0$. Thus we obtain

$$\tau_K = \frac{2K_{K_z}}{K_{K_z} + Q_{K_z}} \quad (18)$$

$$\rho_K = \frac{K_{K_z} - Q_{K_z}}{K_{K_z} + Q_{K_z}}. \quad (19)$$

We find the transmission T_K and reflection R_K coefficients from the probability current, which is given by

$$\mathbf{J} = \frac{1}{2im}(\Psi^*\nabla\Psi - \Psi\nabla\Psi^*). \quad (20)$$

If Q_{K_z} is purely imaginary (i.e., *relatively weaker* strong potential), we get

$$R_K = |\rho_K|^2 = 1, \quad T_K = 0. \quad (21)$$

This is the same result with the intermediate Klein step in 1D. If Q_{K_z} is real, however, the coefficients are

$$T_K = \frac{Q_{K_z}|\tau_K|^2}{K_{K_z}} \quad (22)$$

$$R_K = |\rho_K|^2. \quad (23)$$

Note, since $Q_{K_z} < 0$, the probability is conserved at the expense of a negative transmission coefficient and a reflection coefficient exceeding unity. This paradox can be resolved by employing the notion of particle-antiparticle pair production, due to the strong potential. The antiparticles create a negative charged current moving right inside the potential barrier, while the particles are reflected and combined with the incident beam leading to a positively charged current moving to the left. This is the essence of the peculiarities in equations (22) and (23).

4. Conclusion

We theoretically investigated the underlying physics of similar behaviors resulting from Klein-Gordon and Maxwell's equations in the negative refraction regime. To the best of our knowledge, such a 2D scattering from a semi-infinite Klein step potential is treated here first, inspired by LHMs. The 2D case not only verifies the Klein paradox existing in one dimension, but also manifests the negative refraction phenomenon for matter waves. Based on the analogy described in this letter, we simulated the Klein paradox using LHMs. In fact, although not mentioned above, Fig. 2 is retrieved directly from the LHM simulation in Fig. 1 under certain transformations. Basically, individual Fourier components of the wavepackets in both the LHM and Klein cases are analytically matched. This directly maps the refractive index of the LHM to the Klein potential. A constant Klein potential given by the transformation, despite the inherent dispersion in the LHM, is ensured by the counter-dispersive nature of the mapping that compensates the LHM dispersion. Our work has implications to the analog quantum simulations of many exotic phenomena in the field of relativistic

quantum mechanics with relatively simple optical benchtop experiments, incorporating an appropriate metamaterial design or graphene.

Acknowledgments

Authors would like to thank David R. Smith and Thomas Koschny for inspiring and fruitful discussions. This work was supported in part by the National Security Agency (NSA) and Advanced Research and Development Activity (ARDA) under Army Research Office (ARO) Grant No. DAAD19-01-1-0520, by the DARPA QuIST program under contract F49620-02-C-0010, and by the National Science Foundation (NSF) under grant ECS-0202087.

References

1. Veselago, V. G. The electrodynamics of substances with simultaneously negative values of ϵ and μ . *Sov. Phys. Usp.* **10**, 509–514 (1968).
2. Smith, D. R., Padilla, W. J., Vier, D. C., Nemat-Nasser, S. C., and Schultz, S. Composite medium with simultaneously negative permeability and permittivity. *Phys. Rev. Lett.* **84**, 4184–4187 (2000).
3. Smith, D. R. and Kroll, N. Negative refractive index in left-handed materials. *Phys. Rev. Lett* **85**, 2933–2936 (2000).
4. Shelby, R. A., Smith, D. R., and Schultz, S. Experimental verification of a negative index of refraction. *Science* **292**, 77–79 (2001).
5. C. Enkrich, et al. Magnetic metamaterials at telecommunication and visible frequencies. *Phys. Rev. Lett.* **95**, 203901–203904 (2005).
6. Dolling, G., Enkrich, C., Wegener, M., Soukoulis, C. M., and Linden, S. Low-loss negative-index metamaterial at telecommunication wavelengths. *Opt. Lett.* **31**, 1800–1802 (2006).
7. Dolling, G., Wegener, M., Soukoulis, C. M., and Linden, S. Negative-index metamaterial at 780 nm wavelength. *Opt. Lett.* **32**, 53–55 (2006).
8. U. K. Chettiar, et al. Dual-band negative index metamaterial: double negative at 813 nm and single negative at 772 nm. *Opt. Lett.* **32**, 1671–1673 (2007).
9. W. Cai, et al. Metamagnetics with rainbow colors. *Opt. Express* **15**, 3333–3341 (2007).
10. Ni, G.-J., Zhou, W., and Yan, J. Klein paradox and antiparticle. [arXiv: quant-ph/9905044](https://arxiv.org/abs/quant-ph/9905044).
11. Nitta, H., Kudo, T., and Minowa, H. Motion of a wave packet in the Klein paradox. *Am. J. Phys.* **67**, 966–971 (1999).
12. Calogeracos, A. and Dombey, N. Klein tunnelling and the Klein paradox. *Int. J. Mod. Phys. A* **14**, 631–644 (1999).

13. S. P. Kim and D. N. Page. Schwinger pair production via instantons in strong electric fields. *Phys. Rev. D* **65**, 105002 (2002).
14. Valanju, P. M., Walser, R. M., and Valanju, A. P. Wave refraction in negative-index media: always positive and very inhomogeneous. *Phys. Rev. Lett* **88**, 187401–187404 (2002).
15. Smith, D. R., Schurig, D., and Pendry, J. B. Negative refraction of modulated electromagnetic waves. *Appl. Phys. Lett* **81**, 2713–2715 (2002).
16. Foteinopoulou, S., Economou, E. N., and Soukoulis, C. M. Refraction in media with a negative refractive index. *Phys. Rev. Lett.* **90**, 107402–107405 (2003).
17. Cheianov, V. V., Fal’ko, V., and Altshuler, B. L. The focusing of electron flow and a Veselago lens in graphene p-n junctions. *Science* **315**, 1252–1255 (2006).
18. M. I. Katsnelson, Graphene: carbon in two dimensions. *Materials Today* **10**, 20–27 (2007).
19. Katsnelson, M. I., Novoselov, K. S., and Geim, A. K. Chiral tunnelling and the Klein paradox in graphene. *Nature Phys.* **2**, 620–625 (2006).
20. Dombey, N. and Calogeracos, A. Seventy years of the Klein paradox. *Phys. Reports* **315**, 41–58 (2006).
21. Gingrich, D. M. Physics Lecture Notes: Advanced Quantum Mechanics II, University of Alberta (2001).

List of Figure Captions

Fig. 1. (Color online) Negative refraction of an obliquely incident Gaussian wavepacket at the interface between semi-infinite PIM and NIM media. Arrows indicate the wavevectors for an arbitrary plane wave (\mathbf{K}_L) in the incident wavepacket and its corresponding transmitted (\mathbf{Q}_L) and reflected (\mathbf{K}'_L) wavevectors. They are drawn perpendicular to their respective wavefronts. The colors show the relative intensity pattern at an arbitrary time. Lengths are in SI units. Interference fringes occur due to the incident (bottom left) and reflected (top left) wavepackets near the interface. Transmittance and reflectance at the center frequency, $\omega = 5\text{GHz}$, gives $T_L = 0.855$ and $R_L = 0.145$, respectively, for $\Theta_i = \pi/6$.

Fig. 2. (Color online) Negative refraction of a Gaussian beam of spin-zero particles at the boundary of a strong potential, V , for $z > 0$. \mathbf{K}_K indicates the wave vector of an arbitrary wave component in the incident flux, while \mathbf{Q}_K and \mathbf{K}'_K are the corresponding transmitted and reflected counterparts. The directions of group (\mathbf{V}_g) and phase (\mathbf{V}_p) velocities are antiparallel. The colors show the relative probability density pattern at an arbitrary time. Lengths are in SI units. Transmittance and reflectance are calculated as $T_K = -3.66$ and $R_K = 4.66$, respectively, at the center energy, $E = 20.7\mu\text{eV}$, of the incoming wavepacket, taking $V = 70.63\mu\text{eV}$ and $\Theta_i = \pi/6$.

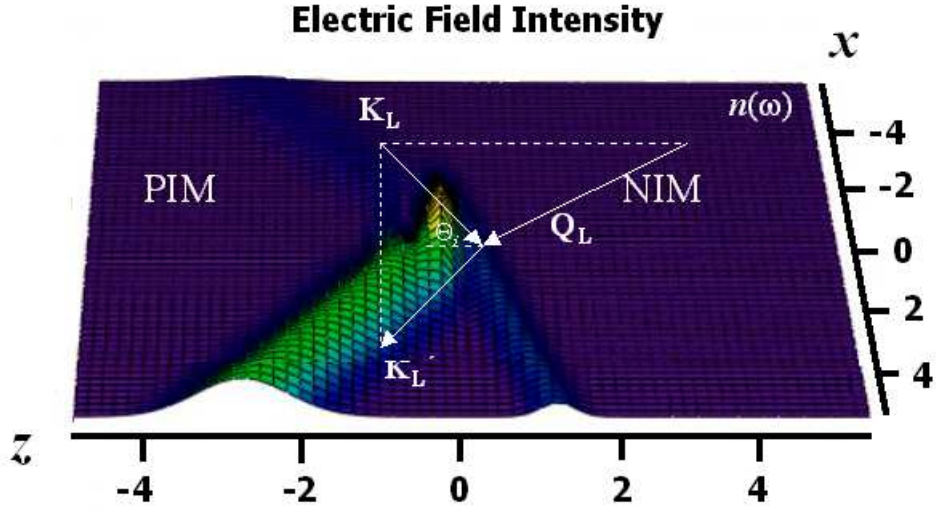


Fig. 1. (Color online) Negative refraction of an obliquely incident Gaussian wavepacket at the interface between semi-infinite PIM and NIM media. Arrows indicate the wavevectors for an arbitrary plane wave (\mathbf{K}_L) in the incident wavepacket and its corresponding transmitted (\mathbf{Q}_L) and reflected (\mathbf{K}'_L) wavevectors. They are drawn perpendicular to their respective wavefronts. The colors show the relative intensity pattern at an arbitrary time. Lengths are in SI units. Interference fringes occur due to the incident (bottom left) and reflected (top left) wavepackets near the interface. Transmittance and reflectance at the center frequency, $\omega = 5\text{GHz}$, gives $T_L = 0.855$ and $R_L = 0.145$, respectively, for $\Theta_i = \pi/6$.

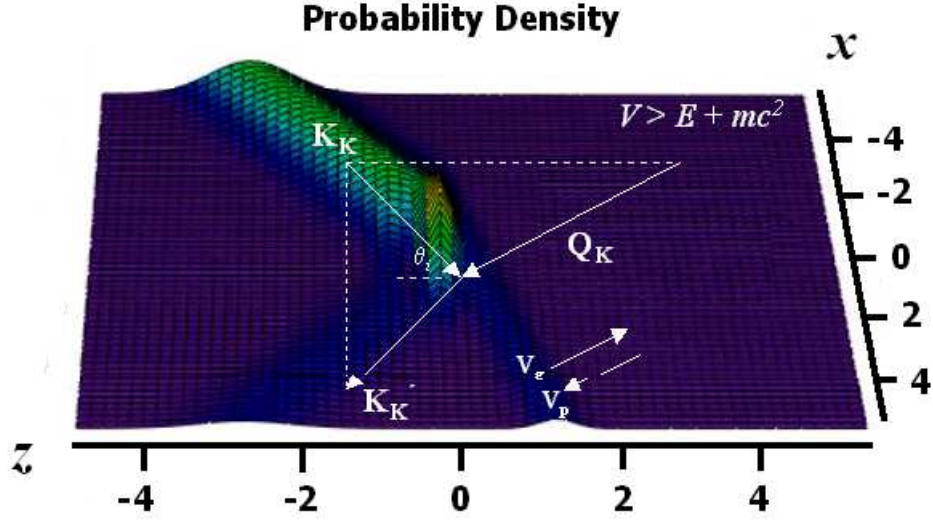


Fig. 2. (Color online) Negative refraction of a Gaussian beam of spin-zero particles at the boundary of a strong potential, V , for $z > 0$. \mathbf{K}_K indicates the wave vector of an arbitrary wave component in the incident flux, while \mathbf{Q}_K and \mathbf{K}'_K are the corresponding transmitted and reflected counterparts. The directions of group (\mathbf{V}_g) and phase (\mathbf{V}_p) velocities are antiparallel. The colors show the relative probability density pattern at an arbitrary time. Lengths are in SI units. Transmittance and reflectance are calculated as $T_K = -3.66$ and $R_K = 4.66$, respectively, at the center energy, $E = 20.7\mu eV$, of the incoming wavepacket, taking $V = 70.63\mu eV$ and $\Theta_i = \pi/6$.